

Simultaneous Measurement of Free-surface and Turbulence Interaction using Specklegram Method and Stereo-PIV

by

G.Tanaka, Y.Ishitsu, K.Okamoto⁽¹⁾ and H.Madarama

Nuclear Engineering Research Laboratory

University of Tokyo

Tokai-mura, Ibaraki 319-1188, JAPAN

⁽¹⁾E-mail: okamoto@utnl.jp

ABSTRACT

The interaction of horizontal jet and free surface was experimentally evaluated, using the Specklegram method and Stereo-PIV. The turbulence at the free surface causes fully three dimensional non-linear phenomena. In order to evaluate the interactions, the three dimensional free surface shape and velocity distribution just beneath the surface should be simultaneously measured. Here, Stereoscopic Particle Image Velocimetry (stereo-PIV) and Specklegram Method (Tanaka et al., 2000) were combined to visualize free surface and underlying turbulence simultaneously. The test section was a rectangular tank having a free surface. A circular nozzle was set horizontally beneath the free surface to form a jet. The jet interacted with the free surface, causing the wavy free surface condition. Two cameras were set beneath the test tank to take the stereoscopic view of the turbulent jet. Three-dimensional velocity distribution beneath the surface was obtained on the horizontal plane. Another camera was used for Specklegram Method which visualizes the three-dimensional surface shape. The combined optical technique enabled to measured the free surface wave quantitatively in a high accuracy. Using this quantitative surface information and velocity distribution measured by stereo-PIV, correlation between free surface fluctuation and flow field was obtained.

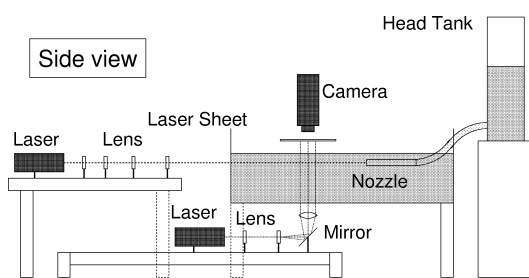


Fig. 1 The camera setup

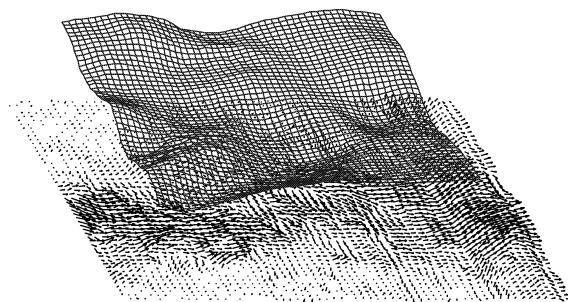


Fig. 2. Instantaneous 3C Velocity and surface shape

1. Introduction

Free surface and its underlying flow field may cause non-linear interaction resulting to phenomena such as self-induced sloshing. Fluctuations by the turbulence affect on free surface, causing the surface shape to be varied. Walker et al.(1995) measured the turbulence near a wavy-free surface using a three-dimensional Laser Doppler Velocimeter (LDV), showing the detailed characteristics of the free surface turbulence. However, their study just measured the averaged liquid velocity perturbation distribution. Since the free surface is a movable boundary condition, the surface response to the disturbance of the liquid is very important. In order to evaluate the interaction between free surface and turbulence, three-dimensional free surface shapes and the three-dimensional velocity distributions beneath the free surface should be simultaneously measured. Several techniques were proposed to measure the free surface shapes using the visualization technique. Suzuki et al.(1995) proposed a photometric stereo technique to visualize the surface gradient. It uses the distorted white light to illuminate the surface. The light was reflected at the surface and was projected to the screen above the surface. Then the intensity distribution on the screen was taken stereoscopic by CCD cameras to be converted to the surface height. Dabiri et al. (2000), applied free surface gradient detector (FSGD) and Digital Particle Image Velocimetry (DPIV) to obtain the correlation between free surface elevation and shear layer. They observed the three-dimensional free surface shape using the FSGD technique, and also simultaneously took the velocity distribution beneath the surface using two-dimensional DPIV. Their result showed the strong correlation between the vorticity distribution and the free surface wave height. There was a highest peak of the wave and the large vorticity at the same point.

In this study, improved Specklegram Method(Tanaka et al., 2000) was applied to visualize the 3-dimensional free surface shape. Specklegram Method uses laser specklegram refraction at the free surface, resulting to a simple measurement setup. Stereoscopic Particle Image Velocimetry (Stereo-PIV) was combined with this Specklegram Method. Using this system, three dimensional free surface shape and three velocity components beneath the free surface was simultaneously measured.

2. Experimental Setup

In order to evaluate the interaction between the free surface and turbulence, the jet was injected horizontally under the free surface. The interaction between the jet and free surface was measured experimentally. Figure 1 shows the schematic of the experimental setup. The test section was a rectangular tank having a free surface. A circular nozzle was set horizontally beneath the free surface to form a jet. The nozzle's inner diameter (D) was 5mm. The center of the nozzle was set 10mm ($2D$) under the free surface. The nozzle axial direction was defined as x-axis. The depth and span-wise directions were defined as z-axis and y-axis respectively. The injected water jet interacted with the free surface, causing the wavy free surface condition. The jet inside the nozzle was fully developed when it reached the end of the nozzle. The head tank was used to supply the constant flow rate. The velocity of the injected jet was set to be 0.75 and 1.0m/s. The Reynolds number in the nozzle was about 3700 and 5000, respectively. ($Re=V_{in} D/\nu$). The water level was kept constant using the overflow at the downstream of the jet. The Froude number with the representative length of the nozzle depth ($H=2D$) was more than 2, showing the wavy surface condition ($Fr=V_{in}/\sqrt{gH}$).

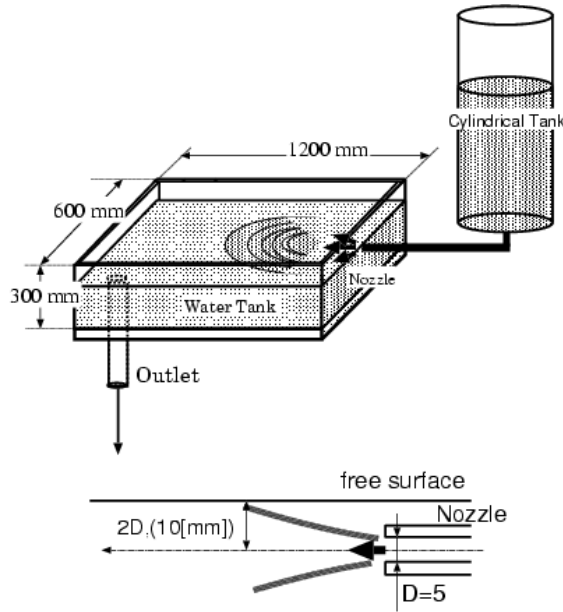


Fig.1 Experimental Setup

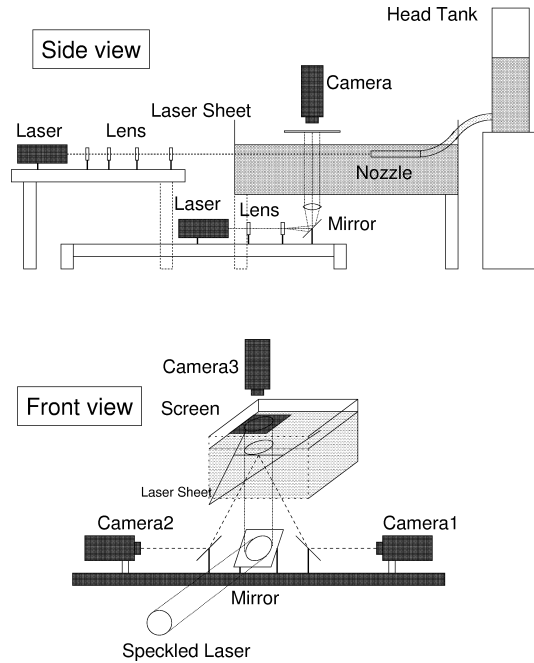


Fig.2 Camera Setup

Optical setup for the visualization was shown in Fig. 2. Cameras 1 and 2 were used for stereo-PIV and viewed the jet through the mirror which was set beneath the test tank. Camera 3 was used for the specklegram measurement. All three camera was the same type of camera, HITACHI KPF-110 (1024 x 1024pixel, 10bit). A parabolic mirror ($\phi=200\text{mm}$) was set beneath the test tank, and was used to reflect the cylindrical laser light for specklegram method to be projected to the screen above the free surface.

2.1 Specklegram Method

In order to measure the three dimensional surface shape, Specklegram Method (Tanaka et al., 2000) was applied. Figure 3 shows the schematic of the speckle measurement. The laser light through the optical fiber system or diffuser contained a lot of speckle noises caused by the small deflection and multi-reflection inside the fiber or diffuser. The speckle noises through the optical fiber or diffuser were applied to the speckle pattern for the surface measurement. From the figure on the left, local surface gradient θ could be written as below:

$$\theta = \frac{\delta}{(n-1)L}$$

where δ was the local displacement vector, n was the refractive index, L was the distance between the surface and the screen. The diameter of the visualized surface area was about 60mm. The speckle pattern projected on the screen was recorded by progressive CCD camera (HITACHI KPF-110, 1024 x 1024pixel, 10bit). An example of the speckle pattern displacement is shown in the right side of Fig. 3. The local displacement (δ) was calculated by comparing the images between without wave (reference) and with wave (object). The cross-correlation technique used in Particle Image Velocimetry was applied to calculate the local displacement of the object image from the reference image. In order to calculate the displacement with

high accuracy, gradient method based sub-pixel analysis (Sugii et al., 2002) was applied. This method based on optical flow technique had an accuracy of 0.01 pixel for sub-pixel analysis of cross correlation PIV technique. Reconstructed surface shape was shown in Fig. 4. The surface was reconstructed from the vectors shown in the right side of Fig. 3.. The wave height was less than 1mm and wave length was about 30mm. It can be clearly seen that the three dimensional surface shape was visualized quantitatively.

The accuracy of the technique was verified by the numerical simulation and verification experiment with the Laser Focus Displacement detector. The specklegram method cannot detect the larger curvature surface, such as breaking wave. However, it can measure the smaller curvature surface with high accuracy.

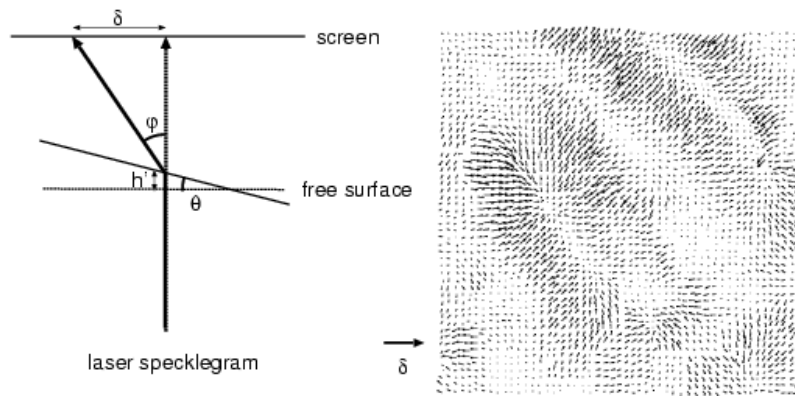


Fig. 3 Specklegram Method

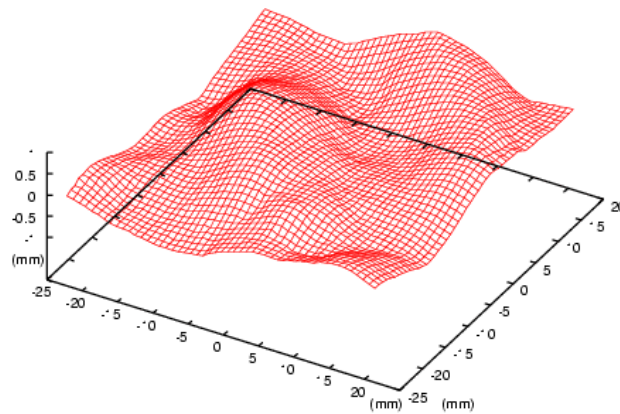


Fig. 4 Example of Reconstructed free-surface (from Fig. 3)

2.2 Stereo Particle Image Velocimetry

In order to obtain the three-dimensional velocity profile on the laser light sheet plane, stereo PIV technique was applied. The camera setup is shown in Fig. 2. These cameras were set in the scheimplug condition (Micro-Nikkor 85mm). The camera was set beneath the test tank and the distance to the target area was about 1500mm. Laser light sheet was generated by a double pulsed 25mJ Nd:YAG laser ($\lambda=532\text{nm}$) horizontally beneath the free surface. The depth of the illumination plan was set to be 10mm, where the depth of the nozzle (H) was also 10mm.

To calibrate the stereo-camera, a gridded stainless plate was used. The calibration plate was 200 x 200mm and had 10000 grid points on the plate. The plate was set at the measuring region and on the laser light sheet plane. The direct mapping method (Soloff et al., 1997) was applied for the camera calibration, using about 6000 grid points. As the mapping function estimate, a least-squares polynomial with cubic dependence in x and y, but quadratic dependence in z was adopted. With the verification, the mapping error was found out to be less than 0.1 pixel at each grid point on the calibration plate.

For the PIV evaluation algorithm, highly accurate sub-pixel analysis based on gradient method (Sugii et al., 2000) was applied for the cross correlation PIV. Also, recursive PIV technique with correlation based error correction (Hart et al., 2000) was applied in order to obtain the velocity vectors with high resolution.

2.3 Simultaneous Measurement Technique

The Simultaneous measurement of the free surface shape and the underlying flow field was realized using these two optical methods mentioned above. Three cameras and two laser units were driven by the pulse generator and the delay generator. The pulse generator had 4 output channels that can produce TTL signals up to 30Hz. These signal were delayed inside the delay generator which had one input channel and 8 output channels. Timing chart of these equipment is shown in Fig.5. The PIV camera opened for the PIV double pulse laser shot, while the specklegram camera closed. On the other hand, the specklegram camera just opened during the PIV camera closing term. The specklegram laser illuminated with synchronizing the specklegram camera. Therefore, the system for PIV measurement and specklegram measurement never had interfered each other.

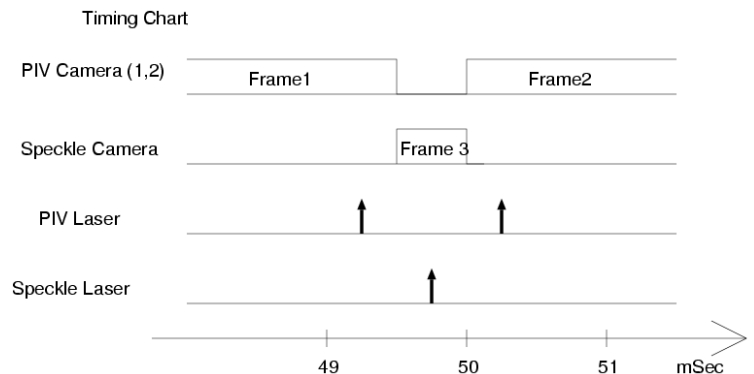


Fig. 5 Laser and Camera Timing Chart

3. Experimental Results

Mean velocity vector distribution is shown in Fig. 6 for the case of $V_{in}=1.0\text{m/s}$. The center of the measuring area was $x=20D$ downstream from the nozzle exit. The mean velocity profile was an average of 144 instantaneous velocity distributions. Using the stereo PIV method, three component of the velocity was obtained at the laser light sheet plane. The jet had a symmetric velocity distribution for the horizontal velocity component. The vertical component of the velocity profile was not symmetric to the laser light plane, and was slightly headed downward. This was because the horizontal jet close to the surface tends to shift toward the free surface.

Figure 7 shows an example of the instantaneous velocity vector with its free surface shape on the top. Three components of the velocity field at the laser light sheet plane and also the surface shape in the same time was quantitatively visualized. It can be clearly seen the jet below generating the surface wave toward the jet's axial direction. The region measured by stereo-PIV was not fully covered by the surface measurement. This results from the optical setup chosen in this experiment. This problem could be easily evaded by choosing a larger lens for the specklegram surface measurement.

Since the vertical component was hard to view on the figure above, Figure 8 shows its vertical velocity component. From the figure meandering of the jet in its horizontal and vertical direction can be clearly seen. For example, the vertical velocity was negatively large at $x=-20\text{mm}$ and $x=10\text{mm}$. The cycle for meandering was about 30mm for both directions. Figure 9 shows the water level, taken simultaneously with the velocity profiles. The peak of the wave can be seen at $(x,y)=(-10,0)\text{mm}$ and also at $(20,10)\text{mm}$. From this figure, the wavelength was estimated to be about 30mm . It agreed well with the observation during the experiment. And it also agrees with the meandering cycle of the jet which was about 30mm . However, peak of the surface wave did not match the peak of the vertical velocity components ($(x,y)=(0,0)\text{mm}$ on Fig.8). The highest peak of the wave was observe at $x=-8\text{mm}$ on Fig.9, but the up-welling velocity of the jet was high at the point of $x=0\text{mm}$ on Fig.8. It can be seen from these figures that there were some phase-lag about 90 degrees between the surface wave and the vertical component of the jet. This value quite agrees with the theoretical value which should be also 90 degrees (i.e., $w=dh/dt$).

Figure 11 shows the correlation for the turbulent fluctuation value, $\frac{(v'^2-w'^2)}{U_{in}^2}$, which represent the

anisotropy condition at free surface. The value denotes the relation between the horizontal (v') and vertical (w') fluctuations. The value was calculated from the Stereo PIV data. When the jet velocity is 1m/s (larger Fr case), the value takes the positive value at the center of the jet. While, it takes negative for the slower velocity, i.e., 0.7m/s (smaller Fr). This value strongly relates to the so called surface current (Walker et al., 1995). They also revealed the similar results using LDV. The surface current will play important role on the free-surface turbulence.

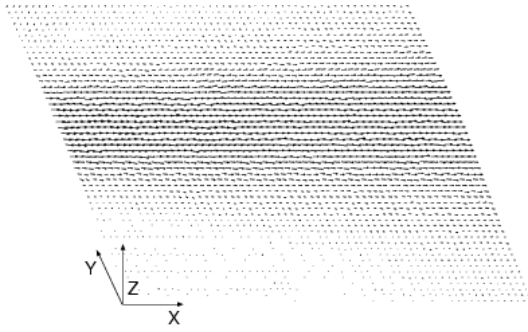


Fig. 6 Mean velocity vectors

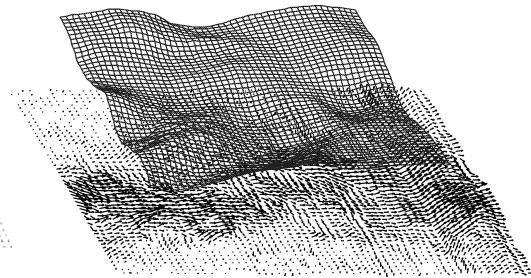


Fig.7 Instantaneous velocity and free-surface

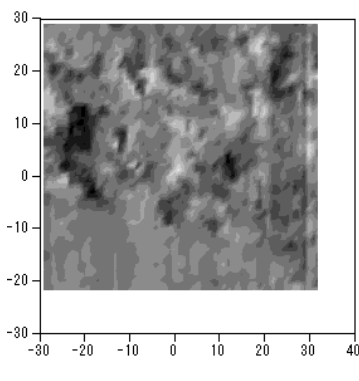


Fig.8 Vertical components of velocity distribution

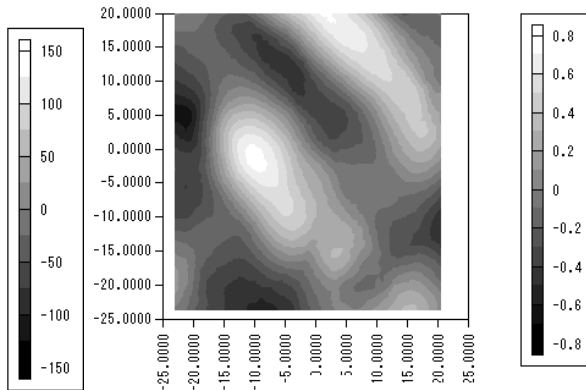
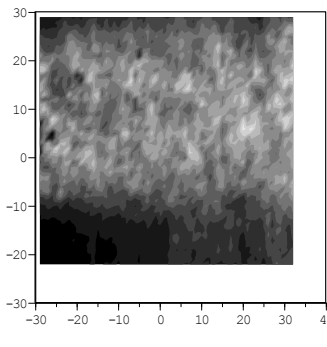
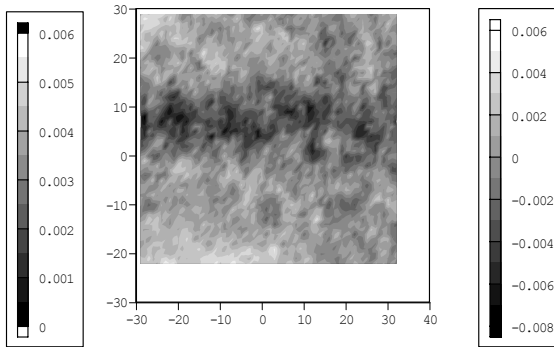


Fig.9 Free surface level



(a) Larger Fr case ($V_{in}=1.0\text{m/s}$)



(b) Smaller Fr case ($V_{in}=0.7\text{m/s}$)

Fig. 10 Surface current related value $\frac{(v^2-w^2)}{U_{in}^2}$

4. Conclusion

Optical technique was developed for the simultaneous measurement of the three-dimensional surface shape and velocity distribution beneath the free surface. Interference of the laser light sheet for stereo-PIV measurement and the volume illumination for Specklegram Method was avoided using the pulsed laser and synchronizing the CCD camera and laser unit. The high resolution CCD camera and the high accuracy sub-pixel analysis enabled the free surface shape and the velocity distribution to be measured simultaneously with high resolution and accuracy. The three-components velocity distribution for horizontal plane at the center of the nozzle, and the three-dimensional free surface shape were obtained. As a result, vertical velocity component of the jet had a strong effect on the free surface waves.

References

- Tanaka, G., Okamoto, K., and Madarame, H., 2000, "Experimental investigation on the interaction between polymer solution jet and free surface," *Experiments in Fluids*, Vol 29-2, pp.178-183.
- Walker, D.T., Chen, C.Y., and Willmarth, W.W., 1995, "Turbulence structure in free-surface jet flows," *Journal of Fluid Mech.*, Vol 291, pp.223-261.
- Suzuki, T., Sumino, K., 1995, "A technique of wave measurement using photometric stereo," *J Vis Soc Japan*, Vol 15, pp.351.
- Dabiri,D., and Gharib,M., 2000, "Interaction of a shear layer with a free surface," *Proc. 9th Int. Symp. on Flow Visualization*, Paper number 72
- Soloff, S.M., Adrian, R.J, and Liu, Z-C., 1997, "Distortion compensation for generalized stereoscopic particle image velocimetry," *Meas. Sci. Technol.*, Vol 8, pp.1441-1454.
- Sugii Y., Nishio S., Okuno T. and Okamoto K., 2000, "A highly accurate iterative PIV technique using a gradient method," *Meas. Sci. Technol.*, Vol 11, pp.1666-1673.
- Hart D.P., 2000, "Super resolution PIV by recursive local correlation," *J. Visualization*, Vol 3, pp.187-194.